ChemComm

# Semiconducting Polymer Dots with Monofunctional Groups



| | |
|---|---|
| Journal: | *ChemComm* |
| Manuscript ID: | CC-COM-03-2014-001689.R1 |
| Article Type: | Communication |
| Date Submitted by the Author: | 04-Apr-2014 |
| Complete List of Authors: | Ye, Fangmao; Department of Chemistry, University of Washington<br>Chiu, Daniel; University of Washington, Chemistry |
| | |

Chemical Communications ChemComm


Cite this: DOI: 10.1039/c0xx00000x

www.rsc.org/xxxxxx

ARTICLE TYPE

# Semiconducting Polymer Dots with Monofunctional Groups

**Fangmao Ye[a], Changfeng Wu[b], Wei Sun[a], Jiangbo Yu[a], Xuanjun Zhang[c], Yu Rong[a], Yue Zhang[a], I-Che Wu[a], Yang-Hsiang Chan[d] and Daniel T. Chiu[a]***

***Received (in XXX, XXX) Xth XXXXXXXXX 20XX, Accepted Xth XXXXXXXXX 20XX***

**DOI: 10.1039/b000000x**

**This communication describes an approach for preparing monovalent semiconducting polymer dots (*m*Pdots) with size of 5nm where each *m*Pdot was composed of precisely a single active functional group.**

Monovalent fluorescent probes with sizes less than 10 nm are desirable for in vitro and in vivo biological applications.[1] Although conventional organic dyes have nanometer sizes and monovalency, they usually suffer from low absorptivity and poor photostability. These drawbacks have limited their application in high-sensitivity imaging techniques and high-throughput assays. Semiconducting quantum dots (Qdots) have been developed as brighter and more photostable probes than conventional organic dyes, but their relatively large hydrodynamic diameter and multivalency are critical constraints for biological applications.[2] Multivalency of Qdots may result in the cross-linking of surface proteins, which can activate signaling pathways and dramatically reduce receptor mobility. As a result, much effort has been devoted in the past several years to develop monovalent Qdots with smaller sizes.[3]

Semiconducting polymer dots (Pdots) have recently emerged as a new group of fluorescent probes which possess large absorption cross-sections, high quantum yields, and fast emission rates.[4] The brightness of Pdots has been shown to be an order of magnitude higher than that of Qdots (e.g. 30 times) of comparable dimensions.[4c, 4i] Moreover, several reports[5] showed that Pdots were nontoxic to cells, an important advantage over Qdots, which can be toxic if heavy metal ions leak from the inorganic core.[6] Finally, Pdots with sizes comparable to typical water-soluble Qdots (~ 15 nm) do not blink, which is an important feature in many single-molecule experiments.

These properties of Pdots make them excellent fluorescent probes for many biological applications. For example, they recently have been used for biological detection,[4l] biosensing platforms,[7]specific cellular[4i] and subcellular targeting and imaging,[8] bioorthogonal labelling,[4j] protein detection[4b] and in vivo tumor targeting. [9] To further optimize Pdots for biological applications, the development of small and monovalent Pdots is the next critical step. Monovalent Pdots (*m*Pdots) have significant advantages over conventional multivalent Pdots because a single functional group is desirable for biological applications that are sensitive to protein/nanoparticle clustering and aggregation. For example, we reported a technique for counting protein copy numbers in synaptic vesicles and subcellular organelles[10] using fluorescent antibodies and single-molecule counting. For these applications, it is imperative that the fluorescent labels do not have excess functional groups that may cause cross-linking and accumulate multiple antibodies per fluorescent label.

Additionally, small Pdots (<10 nm in diameter) are desirable for certain applications. For example, we have recently developed two types of small Pdots (~9 nm), a compact yellow emitting CN-PPV Pdot [8] and a cross-linked Pdot.[11] We found

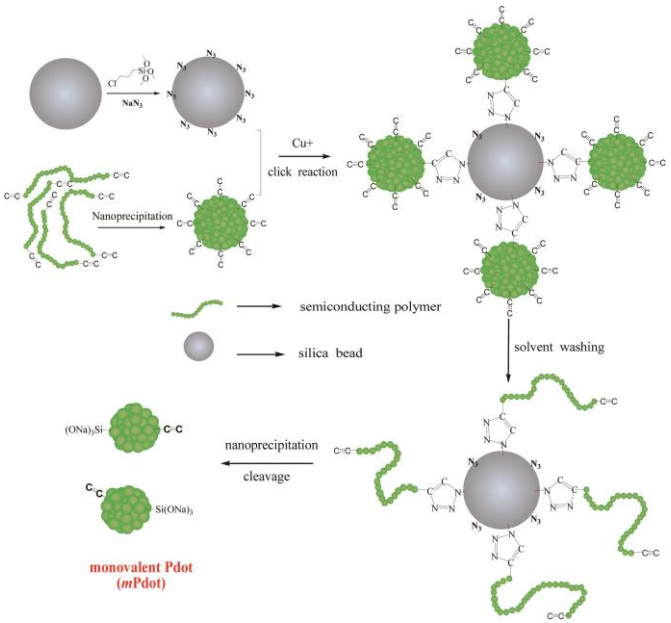


**Figure 1.** The procedure to prepare monovalent Pdots (*m*Pdots). A silica particle with a diameter of ~ 200 nm was prepared and its surface modified with a layer of chloride ($SiO_2$-Cl) via the hydrolysis and condensation of chloridetrimethoxysilane. The $SiO_2$-Cl groups were then modified to azide to form a clickable silica nanoparticle (**ESI**). Separately, regular multivalent PPV-PPA Pdots were prepared using nanoprecipitation (**ESI**); these Pdots had alkyne groups so they could react with the $SiO_2$-$N_3$ on the silica surface via click chemistry. Once the regular PPV-PPA Pdots were clicked onto the surface of the silica nanoparticle, the solvent was changed from aqueous solution to THF and the silica-polymer complex was washed in THF several times. This step removed all the polymer chains in the regular Pdot that were not covalently attached to the silica surface. The single polymer chains attached to the surface of the silica nanoparticles were then re-precipitated into small and monovalent *m*Pdots by re-introducing the silica-polymer complex to aqueous solution from THF. Finally, the *m*Pdots were cleaved from the silica surface and released into solution in the presence of NaOH and Triton 100. To remove NaOH and Triton 100, the *m*Pdot solution was dialyzed overnight in water or buffer.

that these small Pdots were able to label subcellular features more efficiently than larger Pdots (~ 15 nm). For example, microtubules labelled with large Pdots tend to appear spotty in a confocal fluorescence image,[4i] while those same microtubules appear crisp and resolved when labelled with small Pdots.[8,11] Small Pdots also are less prone than large Pdots to alter the diffusional and biological activity of the biomolecules that they label, and small Pdots can access size-restricted cellular regions, such as synapses. To meet these demands for the next generation of Pdots with monovalent functional group and small size, this paper describes an approach based on surface attachment and washing for generating *m*Pdots.

The strategy we developed to prepare *m*Pdots is shown in Fig. 1. Here, we first form Pdots that have multiple polymer chains and are multivalent. We then attach the Pdots onto the surface of silica beads using Click chemistry. Once the Pdots are attached to the bead surface via a functional group (i.e. alkyne group), we wash the bead-Pdot with THF, which causes the Pdot to unfold and the entangled chains to fall apart, leaving a single chain of polymer attached to the bead. Re-introduction of aqueous solution causes the chain to re-collapse to form a single-chain Pdot, and subsequent release of the Pdot from the bead surface results in a monovalent Pdot (**ESI**).

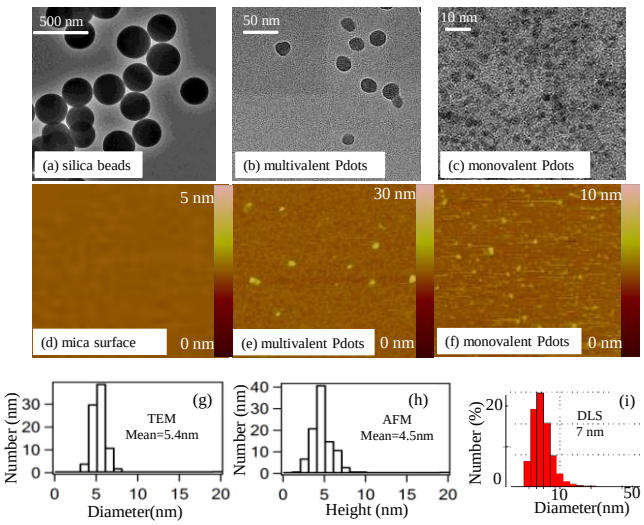


**Figure 2**. Size distribution of *m*Pdots measured with TEM, AFM, and DLS. (a) TEM image of silica beads showing a diameter of ~ 200nm. (b) TEM image of regular PPV-PPA Pdots, which had an average diameter of 34 ± 4 nm, from measurements on 80 Pdots. (c) TEM image of PPV-PPA *m*Pdots. (d) AFM image (1μm × 1μm) of 3-aminopropyltriethoxysilane (APTEOS)-coated mica surface without any nanoparticles. (e) AFM image (0.6μm × 0.6μm) of multivalent regular PPV-PPA Pdots. (f) AFM image (1.2 μm × 1.2 μm) of PPV-PPA *m*Pdots. (g) Size distribution of *m*Pdot shown in (c); average diameter was 5.4 ± 0.5nm from images of 88 *m*Pdots. (h) Height distribution of *m*Pdots measured with AFM; average value was 4.5 ± 0.4nm from measurements on 100 *m*Pdots. (i) DLS result of *m*Pdots in aqueous solution showing a hydrodynamic diameter of 7 nm.

To implement the above strategy, we designed and synthesized a green emitting semiconducting polymer (alkyne terminated linear poly(p-phenylenevinylene) derivative containing two pendent pentaphenylene (PPV-PPA)). The PPV-PPA polymer had only two terminating alkyne click-functional groups (Fig. S1 and S2). And because there was only two alkyne groups in the initial PPV-PPA polymer chain, during the preparation process one of the two alkyne groups was used to covalently bind to the silica surface, and later converted to the terminated $Si(ONa)_3$ group after NaOH cleavage when single chain PPV-PPA was formed. Therefore, there is only one alkyne group left in the single chain PPV-PPA Pdot, resulting in an *m*Pdot with a monovalent alkyne group.

Figure 2 shows the size information for the silica beads, regular PPV-PPA Pdots, and PPV-PPA *m*Pdots. As established by transmission electron microscopy (TEM), the silica bead ($SiO_2$-$N_3$) had a diameter of ~ 200 nm and the regular PPV-PPA Pdot had a 32-nm diameter (Fig. 2a & 2b). A representative TEM image of the *m*Pdots (Fig. 2c) shows that the mean diameter was 5.4 ± 0.5 nm (from 88 *m*Pdots measured; Fig. 2g). Atomic force microscopy (AFM) measurements reported similar results (Fig. 2f); the mean height of *m*Pdots was 4.5 ± 0.4 nm (from 100 *m*Pdots imaged) (Fig. 2h). DLS showed the hydrodynamic diameter of *m*Pdots was 7 nm (Fig. 2i). These three measurements are consistent because the lateral dimension of the collapsed *m*Pdot imaged in TEM should be slightly larger than the height of the collapsed *m*Pdot measured with AFM. The hydrodynamic size is ~1-2 nm larger than TEM and AFM measurements as anticipated because of slight swelling of *m*Pdots in aqueous solution. The molecular weight of PPV-PPA we synthesized was 86,000 g/mol. For a single chain of PPV-PPA that is fully collapsed into a Pdot with a density of ~ 1.0 g/cm$^3$, the resulting *m*Pdot would have a diameter of ~ 6 nm, consistent with the results from both the TEM and AFM experiments.

Our PPV-PPA *m*Pdot had a linear chain polymer with a $Si(ONa)_3$ group on the end of the polymer attached to the silica surface and an alkyne group on the other end. To validate that each *m*Pdot had only a single alkyne functional group, we followed the established approach described in the literature for confirming monovalency of nanoparticles,[12] and carried out two experiments. In the first experiment, we introduced a linker with two azide groups to crosslink *m*Pdots. Figure 3a shows the linker (PEG7-BIS-Azide). If *m*Pdot was monofunctional, then after crosslinking, we expect to see dumb-bell structures (Fig. 3a). If the *m*Pdots had more than one alkyne group, then we should see aggregates of *m*Pdots.

Indeed, regular PPV-PPA Pdots aggregated after the addition of linkers in the presence of freshly prepared copper sulfate (0.5 mM) and L-sodium ascorbate (0.2mM) needed to initiate the click reaction. Before the addition of linker, there was no aggregation, which indicated the aggregation of regular Pdots was only caused by the cross-linking of Pdots triggered by multiple click reactions among the Pdots with multiple alkyne groups. In contrast, when *m*Pdots were used for the same experiment, we observed dumb-bell features (Fig. 3c). As a control, Figure 3b shows a typical image of *m*Pdots when no linker was added but in the presence of 0.5 mM copper sulfate. Figure 3d displays the populations (singular, dumb-bell, or aggregates) of *m*Pdots we observed in the absence and presence of linker: ~ 96% of *m*Pdot was singular when no linker was present (Fig. 3b), but when linker was added, only ~23% of *m*Pdot remained singular and ~ 75% of *m*Pdots formed dumb-bell structures (Fig. 3c). It should be noted that the percentage of dumb-bell structures (~75%) formed by *m*Pdots are similar to that of dumb-bell structures formed by mono functional gold[12b, 12c] or

silver[12a] nanoparticles measured by TEM as reported in literature.[12] We do not expect 100% of *m*Pdots (or other monovalent nanoparticles) to form dumb-bell structures because of reaction kinetics and yield as well as the stoichiometry of linker to *m*Pdots as we will discuss in more detail below. Importantly, we observed almost no Pdot aggregates, thus confirming the absence of multivalent Pdots.

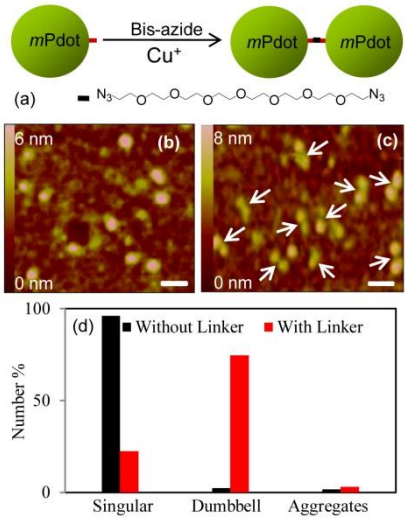


**Figure 3**. Schematic depiction and AFM images showing the formation of dumb-bell structures from crosslinking clickable *m*Pdot with an alkyne group by using α, ω -bis-azide octa(ethylene glycol) (PEG7-Bis-Azide). (a) Chemical structure of PEG7-Bis-Azide and schematic showing the reaction that forms the *m*Pdot dumb-bell features observed in AFM. (b) AFM image showing individual *m*Pdot in the presence of copper sulfate and L-sodium ascorbate but without PEG7-Bis-Azide needed for the click reaction. (c) AFM images of *m*Pdot dumb-bell structures formed in the presence of PEG7-Bis-Azide, copper sulfate, and L-sodium ascorbate; the linker : *m*Pdot ratio used was 1 : 2. The white arrows point to the dumb-bells. Under the same conditions, regular polyvalent Pdots formed aggregates. Scale bars in (b) and (c) represent 20nm. (d) A plot showing the populations of *m*Pdots (singular, dumb-bell, or aggregates) observed in the AFM images in the absence and presence of linker. About 100 Pdots were counted for calculating the percentages.

As additional control, we varied the amount of linker that we added. For the result shown in Figure 3c where most *m*Pdots were in dumb-bell form, the stoichiometry or molar ratio of linker to *m*Pdot was ~ 1:2. When we lowered the molar ratio of linker to *m*Pdot to 1:10, or increased the molar ratio of linker to *m*Pdot to 10:1, the majority of *m*Pdots appeared as a single isolated Pdot (Fig. S3), similar to the image shown in Figure 3b. For linker to *m*Pdot ratio of 1:10, there was simply insufficient linker to form dumb-bell structures, leaving *m*Pdots as isolated nanoparticles. For linker:*m*Pdot ratio of 10:1, we also observed individual isolate *m*Pdots because the reaction between free linker and *m*Pdot was much faster than between *m*Pdot-linker with another *m*Pdot; this difference in reaction kinetics resulted in *m*Pdots all attached to a single linker, which prevented the formation of dumb-bell structures. This set of experiments confirmed each *m*Pdots had only a single functional group.

Next we converted the alkyne functional group on the *m*Pdot to a carboxylic acid group. The motivation for this experiment was two-fold. First, carboxylic acid is one of the most common functional groups used for bioconjugation. We have demonstrated its utility in our past experiments for covalently linking a wide range of biomolecules and dyes to Pdots and transforming it into other functional groups.[4i, 4j, 7] Therefore, this experiment acted as a gateway for changing the alkyne group to other functional groups or for attachment to biomolecules. Second, we had previously demonstrated $Cu^{2+}$ could crosslink Pdots with carboxyl groups because $Cu^{2+}$ is complexed by the carboxyl groups.[13] Monovalent carboxyl *m*Pdots should also form dumb-bell structures in the presence of $Cu^{2+}$ while polyvalent Pdots would form aggregates as we had previously demonstrated(Fig. 4a).[13] This experiment served as another validation that *m*Pdots were monovalent.

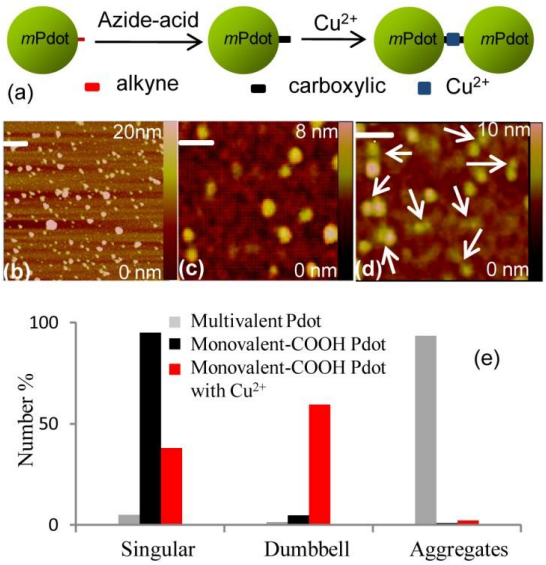


**Figure 4**. Generation of carboxyl-terminated *m*Pdots and the formation of carboxyl *m*Pdot dumb-bells in the presence of $Cu^{2+}$. (a) Schematic showing the transformation of alkyne to carboxylic *m*Pdot and then cross-linking *m*Pdot-COOH to form dumb-bell structures. (b) AFM image of regular polyvalent carboxyl Pdots, formed from alkyne Pdots using azide-acid, in the presence of 0.5 mM $Cu^{2+}$ in HEPES buffer (pH=7.4); only aggregates were observed. (c) AFM image of *m*Pdot with carboxyl group in HEPES buffer (pH=7.4) but without $Cu^{2+}$. (d) AFM image of *m*Pdot with carboxyl group in the presence of 10 mM $Cu^{2+}$ in HEPES buffer (pH=7.4). The white arrows point to the dumb-bell structures. Scale bars in (b), (c), and (d) represent 100nm, 25nm, and 20nm, respectively. (e) A plot showing the populations of regular multivalent Pdots and *m*Pdots (singular, dumb-bell, or aggregates) in the AFM images in the absence and presence of $Cu^{2+}$. About 100 Pdots were counted for calculating the percentages.

To form *m*Pdot-COOH, we used azide-PEG-COOH to react with *m*Pdot-alkyne via click cycloaddition in the presence of copper sulfate (0.5 mM) and L-sodium ascorbate (0.2 mM). Regular multivalent Pdots had a high density of alkyne groups on the surface and quickly aggregated in the presence of copper sulfate when the alkyne groups were transformed to COOH groups (Fig. 4b). The solution turned cloudy. Under the same conditions, *m*Pdots did not aggregate and the solution remained clear. We then dialyzed out the remaining copper (I)/(II) in the *m*Pdot solution and added a more concentrated $Cu^{2+}$ solution at 10 mM to induce *m*Pdots to form dumb-bell structures. Figure 4d shows the result, in which dumb-bell features can be clearly discerned. No aggregates of *m*Pdots were detected, even at 10 mM of $Cu^{2+}$; we note for regular Pdots with COOH groups, only ~ 5 μM of $Cu^{2+}$ was sufficient to induce significant Pdot

aggregations.[13] Figure 5e shows the populations of *m*Pdot (singular, dumb-bell, or aggregates) in the AFM images : ~ 94% of multivalent Pdots was observed to form aggregates in the presence of $Cu^{2+}$, but for *m*Pdots in the presence of $Cu^{2+}$, they formed dumb-bell structures instead (60%). Some *m*Pdots remained singular (38%), likely because $Cu^{2+}$ is not as strong a cross linker and the stability of two Pdots linked by a single $Cu^{2+}$ ion is rather low and prone to disruption. In fact, $Cu^{2+}$ attached to a single carboxyl group is not stable and two carboxyl groups are required to form a stable complex, which also explains why having more $Cu^{2+}$ than *m*Pdots in solution did not prevent formation of dumb-bell structures. From these experiments, the strong contrast in the behavior of regular multivalent Pdots and *m*Pdots is evident.

Finally, we investigated the stability of *m*Pdots in different buffer solutions. Figure S4 showed the normalized fluorescence intensity of *m*Pdots in different buffers (including TRIS, TBE, PBS and HEPES buffer) as a function of time. The result indicated that the fluorescence of the *m*Pdots buffer solution did not change over a period of three days. Because any aggregation of Pdots would result in a decrease in the measured fluorescence intensity due to self quenching,[14] this result confirmed the Pdots are well dispersed and stable over this period, which is suitable for biological applications.

In conclusion, we have developed a method for preparing monovalent and very small Pdots. We carried out two experiments to show that *m*Pdots only had a single functional group. When the *m*Pdots were crosslinked, they formed dumb-bell structures as seen by AFM. We generated clickable *m*Pdots as well as *m*Pdots with a single carboxyl group, which could be used for covalent attachment of a broad range of biological molecules. The importance of having monovalency has been illustrated in the literature for other nanoparticles. For example, monovalent nanoparticles have been shown to label glutamate receptors at neuronal synapses without activating EphA3 tyrosine kinase[3b] while polyvalent nanoparticles result in activation. Monovalent nanoparticles have also been shown to offer improved quantification in tumor targeting and imaging,[3a] and better performance in the tracking of individual proteins in live cells.[15] The development of the very small and monovalent *m*Pdots, coupled with the high brightness of Pdots as we have previously demonstrated,[4c, 4i] is expected to advance their adoption as a useful fluorescent probe in biomedical applications. You can also put lists into the text

## Notes and references

[a] Department of Chemistry, University of Washington, Seattle, Washington 98195, United States
[b] Present address: State Key Laboratory on Integrated Optoelectronics, College of Electronic Science and Engineering, Jilin University, Changchun, Jilin 130012, China
[c] Present address: Division of Molecular Surface Physics & Nanoscience, Department of Physics, Chemistry, and Biology, Linköping University, Linköping 58183, Sweden
[d] Present address: Department of Chemistry, National Sun Yat-Sen University, Kaohsiung, Taiwan

† Electronic Supplementary Information (ESI) available: materials, characterization and Pdots preparation. See DOI: 10.1039/b000000x/

[1] aS. A. Hilderbrand, K. A. Kelly, R. Weissleder, C.-H. Tung, *Bioconjugate Chemistry* **2005**, *16*, 1275-1281; bF. Shao, R. Weissleder, S. A. Hilderbrand, *Bioconjugate Chemistry* **2008**, *19*, 2487-2491; cW. Shi, S. Dolai, S. Rizk, A. Hussain, H. Tariq, S. Averick, W. L'Amoreaux, A. El Idrissi, P. Banerjee, K. Raja, *Organic Letters* **2007**, *9*, 5461-5464; dS. Wu, C. Zhu, C. Zhang, Z. Yu, W. He, Y. He, Y. Li, J. Wang, Z. Guo, *Inorganic Chemistry* **2011**, *50*, 11847-11849.

[2] D. R. Larson, W. R. Zipfel, R. M. Williams, S. W. Clark, M. P. Bruchez, F. W. Wise, W. W. Webb, *Science* **2003**, *300*, 1434-1436.

[3] aH. Y. Liu, X. Gao, *Bioconjugate Chemistry* **2011**, *22*, 510-517; bM. Howarth, W. Liu, S. Puthenveetil, Y. Zheng, L. F. Marshall, M. M. Schmidt, K. D. Wittrup, M. G. Bawendi, A. Y. Ting, *Nat. Meth.* **2008**, *5*, 397-399.

[4] aX. Zhang, J. Yu, Y. Rong, F. Ye, D. T. Chiu, K. Uvdal, *Chem. Sci.* **2013**, *4*, 2143-2151; bF. Ye, P. B. Smith, C. Wu, D. T. Chiu, *Macromolecular Rapid Communications* **2013**, *34*, 785-790; cC. Wu, D. T. Chiu, *Angew. Chem., Int. Ed.* **2013**, *52*, 3086-3109; dW. Sun, J. Yu, R. Deng, Y. Rong, B. Fujimoto, C. Wu, H. Zhang, D. T. Chiu, *Angew. Chem., Int. Ed.* **2013**, *52*, 11294-11297; eY. Rong, C. Wu, J. Yu, X. Zhang, F. Ye, M. Zeigler, M. E. Gallina, I.-C. Wu, Y. Zhang, Y.-H. Chan, *ACS nano* **2013**, *7*, 376-384; fC. Zhu, L. Liu, Q. Yang, F. Lv, S. Wang, *Chemical Reviews* **2012**, *112*, 4687-4735; gK. Li, B. Liu, *Journal of Materials Chemistry* **2012**, *22*, 1257-1264; hS. Das, A. M. Powe, G. A. Baker, B. Valle, B. El-Zahab, H. O. Sintim, M. Lowry, S. O. Fakayode, M. E. McCarroll, G. Patonay, M. Li, R. M. Strongin, M. L. Geng, I. M. Warner, *Anal. Chem.* **2012**, *84*, 597-625; iC. Wu, T. Schneider, M. Zeigler, J. Yu, P. G. Schiro, D. R. Burnham, J. D. McNeill, D. T. Chiu, *J. Am.Chem. Soc.* **2010**, *132*, 15410-15417; jC. Wu, Y. Jin, T. Schneider, D. R. Burnham, P. B. Smith, D. T. Chiu, *Angew. Chem., Int. Ed.* **2010**, *49*, 9436-9440; kJ. Pecher, S. Mecking, *Chemical Reviews* **2010**, *110*, 6260-6279; lC. Wu, B. Bull, C. Szymanski, K. Christensen, J. McNeill, *ACS Nano* **2008**, *2*, 2415-2423.

[5] aL. P. Fernando, P. K. Kandel, J. Yu, J. McNeill, P. C. Ackroyd, K. A. Christensen, *Biomacromolecules* **2010**, *11*, 2675-2682; bN. A. A. Rahim, W. McDaniel, K. Bardon, S. Srinivasan, V. Vickerman, P. T. C. So, J. H. Moon, *Advanced Materials* **2009**, *21*, 3492-3496; cK. Y. Pu, K. Li, J. B. Shi, B. Liu, *Chemistry of Materials* **2009**, *21*, 3816-3822.

[6] R. Hardman, *Environ Health Perspect* **2006**, *114*, 165-172.

[7] aF. Ye, C. Wu, Y. Jin, Y.-H. Chan, X. Zhang, D. T. Chiu, *J. Am.Chem. Soc.* **2011**, *133*, 8146-8149; bY.-H. Chan, C. Wu, F. Ye, Y. Jin, P. B. Smith, D. T. Chiu, *Anal. Chem.* **2011**, *83*, 1448-1455.

[8] F. Ye, C. Wu, Y. Jin, M. Wang, Y.-H. Chan, J. Yu, W. Sun, S. Hayden, D. T. Chiu, *Chem. Comm.* **2012**, *48*, 1778-1780.

[9] C. Wu, S. J. Hansen, Q. Hou, J. Yu, M. Zeigler, Y. Jin, D. R. Burnham, J. D. McNeill, J. M. Olson, D. T. Chiu, *Angew. Chem., Int. Ed.* **2010**, *50*, 3430-3434.

[10] aS. A. Mutch, P. Kensel-Hammes, J. C. Gadd, B. S. Fujimoto, R. W. Allen, P. G. Schiro, R. M. Lorenz, C. L. Kuyper, J. S. Kuo, S. M. Bajjalieh, D. T. Chiu, *The Journal of Neuroscience* **2011**, *26*, 1461-1470; bS. A. Mutch, B. S. Fujimoto, C. L. Kuyper, J. S. Kuo, S. M. Bajjalieh, D. T. Chiu, *Biophysical journal* **2007**, *92*, 2926-2943.

[11] J. Yu, C. Wu, X. Zhang, F. Ye, M. E. Gallina, Y. Rong, I. C. Wu, W. Sun, Y.-H. Chan, D. T. Chiu, *Advanced Materials* **2012**, *24*, 3498-3504.

[12] aB. VIckova, M. Moskovits, I. Pavel, K. Siskova, M. Sladkova, M. Slouf, *Chemical Physics Letters* **2008**, *455*, 131-134; bX. Liu, J. G. Worden, Q. Dai, J. Zou, J. Wang, Q. Huo, *Small* **2006**, *2*, 1126-1129; cJ. G. Worden, Q. Dai, A. W. Shaffer, Q. Huo, *Chemistry of Materials* **2004**, *16*, 3746-3755.

[13] Y. Chan, Y. Jin, C. WU, D. T. Chiu, *Chem. Comm.* **2010**, *47*, 2820-2822.

[14] Y. Jin, F. Ye, C. Wu, Y.-H. Chan, D. T. Chiu, *Chem. Comm.* **2012**, *48*, 3161-3163.

[15] S. Clarke, F. Pinaud, O. Beutel, C. You, J. Piehler, M. Dahan, *Nano Letters* **2010**, *10*, 2147-2154.